Journal of Ginseng Research 46 (2022) 126–137

Contents lists available at ScienceDirect

Journal of Ginseng Research

journal homepage: https://www.sciencedirect.com/journal/journal-of-ginseng-research

Research Article

Oral administration of Jinan Red Ginseng and licorice extract mixtures ameliorates nonalcoholic steatohepatitis by modulating lipogenesis

Daram Yang [a, 1], Hyuneui Jeong [a, 1], Seung-Mi Hwang [b, c, 1], Jong-Won Kim [a], Hee-Won Moon [a], Ye-Eun Lee [b], Hyo-Bin Oh [b, c], Chung-berm Park [b, **], Bumseok Kim [a, *]

[a] Biosafety Research Institute and Laboratory of Pathology, College of Veterinary Medicine, Jeonbuk National University, Iksan-si, Jeollabuk-do, Republic of Korea
[b] Department of Efficacy Study, Institute of Jinan Red Ginseng, Jinan-gun, Jeollabuk-do, Republic of Korea
[c] Department of Food Science and Technology, Jeonbuk National University, Deokjin-gu, Jeonju-si, Jeollabuk-do, Republic of Korea

ARTICLE INFO

Article history:
Received 17 March 2021
Received in revised form
11 May 2021
Accepted 12 May 2021
Available online 21 May 2021

Keywords:
Jinan Red Ginseng
Licorice
Mice
Nonalcoholic steatohepatitis

ABSTRACT

Background: Nonalcoholic steatohepatitis (NASH) is one of the main chronic liver diseases. NASH is identified by lipid accumulation, inflammation, and fibrosis. Jinan Red Ginseng (JRG) and licorice have been widely used because of their anti-inflammatory and hepatoprotective effects. Hence, this study assessed JRG and licorice extract mixtures' effects on NASH progression.
Methods: Palmitic acid (PA) and the western diet (WD) plus, high glucose-fructose water were used to induce *in vitro* and *in vivo* NASH. Mice were orally administered with JRG-single (JRG-S) and JRG-mixtures (JRG-M; JRG-S + licorice) at 0, 50, 100, 200 or 400 mg/kg/day once a day during the last half-period of diet feeding.
Results: JRG-S and JRG-M reduced NASH-related pathologies in WD-fed mice. JRG-S and JRG-M consistently decreased the mRNA level of genes related with inflammation, fibrosis, and lipid metabolism. The treatment of JRG-S and JRG-M also diminished the SREBP-1c protein levels and the p-AMPK/AMPK ratio. The FAS protein levels were decreased by JRG-M treatment both *in vivo* and *in vitro* but not JRG-S.
Conclusion: JRG-M effectively reduced lipogenesis by modulating AMPK downstream signaling. Our findings suggest that this mixture can be used as a prophylactic or therapeutic alternative for the remedy of NASH.

1. Introduction

A western lifestyle and an unhealthy diet are closely related with an increasing prevalence of obesity, metabolic disorder, and cardiovascular disease. Such metabolic abnormalities induce mild liver injury, leading to the onset of nonalcoholic fatty liver disease (NAFLD) [1]. NAFLD is one of the main chronic liver disorders, and its prevalence is gradually increasing among obese people worldwide [2]. The NAFLD spectrum includes simple steatosis and nonalcoholic steatohepatitis (NASH), as well as advanced liver fibrosis, cirrhosis, and hepatocellular carcinoma. Along this spectrum, NASH is an intermediate stage of progressive lesion that is accompanied by hepatocellular damage, metabolic inflammation, and fibrosis [3,4].

Several hypothetical mechanisms have been suggested to describe the development and progression of NASH. One of them has indicated that abnormal lipid metabolism and chronic free fatty acid (FFA) overload can trigger changes from simple steatosis to NASH by inducing hepatocyte death-mediated chronic liver injury, which is closely related with the progression of inflammation and fibrogenesis in the liver [5]. It has been well-documented that Kupffer cells (KCs) and monocyte-derived macrophages have a critical function in NASH-related inflammation and fibrosis. The activation status of these cells is changed during NASH progression, depending upon the degree of stimuli, such as damaged associated molecular patterns, cytokines, gut microbiota-derived endotoxin, and lipid metabolites [6,7]. Hence, many factors and signaling

* Corresponding author. Biosafety Research Institute and Laboratory of Pathology, College of Veterinary Medicine, Jeonbuk National University, 79 Gobong-ro, Iksan-si, Jeollabukdo, 54596, Republic of Korea.
** Corresponding author. Institute of Jinan Red Ginseng, 41 Hongsamhanbang-ro, Jinan-gun, Jeollabuk-do, 55442, Republic of Korea.
E-mail addresses: pcbberm@ijrg.re.kr (C.-b. Park), bskims@jbnu.ac.kr (B. Kim).
[1] These authors contributed equally to this work.

https://doi.org/10.1016/j.jgr.2021.05.006

pathways that are attributable to NASH pathogenesis have been investigated to discover new therapeutic targets.

Panax ginseng has been used as an oriental herbal remedy for more than 2,000 years in Eastern Asia. Among the several types of ginseng, Korean Red Ginseng (KRG, *Panax ginseng* Meyer) is made through a steaming and drying process. KRG has fewer side effects and has more effective pharmacological activities as compared to the original ginseng or its-dried form, called white ginseng [8,9]. It has been demonstrated that KRG has ameliorative effects in various pathologic conditions, such as immune enhancement, alleviation of fatigue, antidiabetic, antistress, antiinflammatory, and antioxidative, as well as several types of organ injuries [10–13]. Also, Jinan Red Ginseng (JRG) extracted from KRG has suppressive effects on fatty acid synthesis in adipocytes or triglyceride synthesis in hepatoma cells [14].

Previous studies have suggested that a mixture of KRG and other botanical therapeutic ingredients such as coffee, puer tea, buckwheat or licorice (*Glycyrrhiza uralensis* Fischer) have complex enhancement effects on various indices related to antioxidative, antibacterial, antiobesity, or collagenase inhibitory activity [15–18]. Among them, glycyrrhizin, a constituent of licorice, has a sweet taste and is known to have antiobesity effects and to alleviate allergy asthma [17,19]. Thus, we herein developed a promising new herbal medicine, a mixture of JRG and licorice, and we evaluated the hepatoprotective effects of this mixture in the NASH model.

2. Materials and methods

2.1. Material preparation

JRG (*Panax ginseng* Meyer) used in the study was 6-years root harvested in Jinan-gun, Jeollabuk-do, Korea. Licorice (*Glycyrrhiza uralensis* Fischer) used in the study was 3-years root harvested in Jecheon-si, Chungcheongbuk-do, Korea. After adding 600 mL of 50% ethanol (EtOH) to 60 g of raw material powder, it was immersed, heated to 80°C, and filtered (Grade 41 Fast Ashless Filter Paper, 20 μm, 1441-125, Whatman). Thereafter, samples were obtained through vacuum concentration (N-1110, EYELA) and freeze drying (FD8512, Freeze Dryer, ilShin BioBase). Contents of main ginsenosides contained in JRG extract and glycyrrhizin contained in licorice extract in 50% EtOH are described in Supplementary Table 1.

2.2. Cell viability assay

Alpha mouse liver 12 (AML-12) cells were cultured in a 96-well plate (1×10^4 cells/well) in Dulbecco's modified Eagle's medium/Ham's F12 (DMEM/F12; Corning, NY, USA) containing 10% fetal bovine serum (FBS; MP Biomedicals, Santa Ana, USA), 1% Insulin–Transferrin–Selenium–Pyruvate (ITSP; Welgene, Gyeongsan, Korea), 40 ng/mL of dexamethasone (Sigma–Aldrich, MO, USA), and an antibiotic-antimycotic solution (Welgene) at 37°C in controlled atmosphere with 5% CO_2. The next day, 10:0, 7:3, 5:5, 3:7, or 0:10 ratios of JRG:licorice at 1 μg/mL were placed into cells with or without 0.4 mM palmitic acid (PA; Sigma-Aldrich) and incubated for 24 hours. Afterward, cell viability was measured by Cell Counting Kit-8 (CCK-8; Dojindo Molecular Technologies, MD, USA), using EMax spectrophotometer (Molecular Devices, CA, USA).

2.3. Cell culture and induction of in vitro NASH model

AML-12 cells and RAW 264.7 cells were cultured into a 12-well plate (5×10^5 cells/well) and were co-cultured in a 12-well insert plate (NEST, Jiangsu, China) at a 2:1 ratio of AML-12:RAW 264.7 in DMEM/F12 (Corning) containing 10% FBS (MP Biomedicals), 1% ITSP (Welgene), 40 ng/mL of dexamethasone (Sigma-Aldrich), and antibiotic-antimycotic solution (Welgene) at 37°C in controlled atmosphere with 5% CO_2. An *in vitro* NASH model was established by treatment of 0.4 mM PA (Sigma-Aldrich) to cells as previously described [20]. Cells were maintained for 24 hours after treatment with a different concentration of JRG-S or JRG-M (0, 10 ng/mL, 100 ng/mL, or 1 μg/mL).

2.4. Animals and experimental design

Six-week-old male C57BL/6J mice were obtained from Taconic Farms, Inc. (DBL Co., Ltd. Eumseong, Korea). The animals were housed at 24 ± 3°C and 50 ± 5% humidity with *ad libitum* access to sterilized normal diet and water during the acclimatization period of one week. This study was approved by the Animal Care and Ethics Committees of Jeonbuk National University (CBNU 2020-082).

We divided the mice into 10 groups of eight mice each: (1) a normal diet (ND; with normal water); (2) a western diet (WD; 40 kcal% fat, 20 kcal% fructose, and 2% cholesterol with high fructose-glucose water [23.1 g d-fructose/L + 18.9 g d-glucose/L]) as previously described [21]; (3) a WD with JRG-S at 50 mg/kg/day (S 50), 100 mg/kg/day (S 100), 200 mg/kg/day (S 200), or 400 mg/kg/day (S 400); (4) a WD with JRG-M at 50 mg/kg/day (M 50), 100 mg/kg/day (M 100), 200 mg/kg/day (M 200), or 400 mg/kg/day (M 400). We gave them either a ND or a WD for 16 weeks. After eight weeks of WD feeding, we orally administered JRG-S and JRG-M dissolved in saline once daily, five days a week, from week nine to 16 to each WD diet-fed group. We measured the body and liver weights at necropsy.

2.5. Serum and hepatic biochemical analysis

The serum biochemistry levels, such as alanine aminotransferase (ALT) and aspartate aminotransferase (AST), were evaluated by an AM101-K assay kit (ASAN Pharmaceutical, Seoul, Korea). Hepatic triglyceride (TG) and total cholesterol (TC) levels were determined by an AM202-K assay kit (ASAN Pharmaceutical) according to the manufacturer's instruction.

2.6. Histopathology and staining analysis

Liver samples of each experimental group were carefully removed and immersed in 10% formalin for tissue fixation. Paraffin-embedded liver was sectioned by a microtome (HM-340E, Thermo Fisher Scientific, MA, USA). We stained the sections with hematoxylin & eosin (H&E) in accordance with typical protocol. To confirm NASH severity, an NAFLD activity score (NAS) system was obtained in accordance with the criteria by Kleiner et al [22].

To detect the apoptosis in the liver, we carried out a terminal deoxynucleotidyl transferase-mediated dUTP nick-end labeling (TUNEL) assay on the paraffin-embedded sections, using an ApopTag Peroxidase *in situ* apoptosis detection kit (EMD Millipore, CA, USA).

To assess the severity of fibrosis, we did sirius red staining of the liver sections with Direct Red 80 (Sigma-Aldrich). We also did Oil-Red O staining (ScyTek Laboratories, UT, USA) using frozen liver tissue sections or cultured cells to determine intracellular lipid accumulation. We evaluated the stained liver section or cell images using light microscopy (BX53F, Olympus Corp., Tokyo, Japan) and digital image software (cellSens Standard, Olympus Corp.). The data is expressed as the mean of each positively stained area per field in the livers or cells.

2.7. Quantitative real time-polymerase chain reaction (qRT-PCR)

The total RNA was extracted from the liver tissue or cells using RiboEx (GeneAll Biotechnology Co. Ltd., Seoul, Korea) and the Hybrid-R RNA purification kit (GeneAll Biotechnology Co. Ltd.). For degradation of DNA, DNase I containing RNase inhibitor (TOYOBO, Osaka, Japan) was added to total RNA. Complementary DNA was synthesized using ReverTra Ace qPCR RT Master Mix (TOYOBO) in accordance with the manufacturer's recommendation. Next, qRT-PCR was conducted with a CFX96 Real-Time PCR Detection System (Bio-Rad Laboratories, CA, USA) using SYBR Green Master Mix (TOYOBO). The relative mRNA concentrations were calculated to that of glyceraldehyde 3-phosphate dehydrogenase (GAPDH). All used primer sequences are shown in Supplementary Table 2.

2.8. Enzyme-linked immunosorbent assay (ELISA)

To confirm the protein levels of proinflammatory cytokines like tumor necrosis factor-alpha (TNF-α) and interleukin-6 (IL-6), cell supernatant was collected and measured by the ELISA kits (Invitrogen, CA, USA) in accordance with the manufacturer's protocol. If this was lower than the minimum measurable value of detection kit, it was expressed as “below the detection limit (B.D.)”.

2.9. Western blot assay

Liver tissues or cultured cells were lysed in a protein extraction reagent (Thermo Fisher Scientific). Protein extracts were obtained by centrifugation at 13,000 × g for 15 minutes at 4°C. Protein concentration was measured with the Pierce BCA Protein Assay kit (Thermo Fisher Scientific). Protein samples were electrophoresed on SDS-PAGE gel, and then transferred to a polyvinylidene difluoride membrane that activated with methanol. The membrane was blocked with Superblock (Thermo Fisher Scientific) for one hour at room temperature and incubated overnight at 4°C of the following primary antibodies: phospho-AMP-activated protein kinase (p-AMPK), AMPK (Cell Signaling Technology, MA, USA), sterol regulatory element-binding protein-1c (SREBP-1c), fatty acid synthase (FAS), and β-actin (Santa Cruz Biotechnology, CA, USA). Secondary horseradish peroxidase-conjugated IgG antibodies (Enzo Life Sciences, NY, USA) were used, and incubated for two hours at room temperature. Protein activities were visualized by the Western ECL Kit (LPS solution, Daejeon, Korea) and ImageQuant LAS 500 (GE Healthcare Life Science, PA, USA). Image analysis for determining relative intensity was conducted using ImageQuant TL software version 8.1 (GE Healthcare Life Science).

2.10. Statistical analysis

All data was presented as means ± standard deviation (SD). Statistical difference between the groups was analyzed by One-way analysis of variance (ANOVA) using Prism version 8.0.1 (GraphPad Software, CA, USA). Liver histopathological assessment was performed using the Kruskal-Wallis nonparametric test, followed by Dunn's multiple comparisons test. The data was shown as being in the median ± interquartile range. A p-value of 0.05 or less was regarded to be statistically significant.

3. Results

3.1. Mixtures of JRG/licorice extracts (7:3) increase cell viability in PA-treated cells

Various ratios of JRG/licorice extracts (10:0, 7:3, 5:5, 3:7, or 0:10) were treated to PA-treated AML-12 cells with the maximum concentration that had not been cytotoxic (1 μg/mL; supplementary Fig. 1A and 1B) for 24 hours. The cell viability was significantly increased in all groups except for the JRG/licorice extract 0:10 ratio group as compared to the PA only-treated group ($p < 0.05$) (supplementary Fig. 1C), and the 7:3 ratio group showed the highest cell viability among them ($p < 0.001$). Therefore, we prepared the JRG/licorice extract mixtures that we used in the *in vivo* and *in vitro* studies in a 7:3 ratio.

3.2. JRG-S or JRG-M decreased PA-induced lipotoxicity in vitro

Representative figures of Oil Red-O stained AML-12 cells and their positive area measurements showed that JRG-S or JRG-M significantly decreased the lipid accumulation at 100 ng/mL and 1 μg/mL of both the JRG-S and JRG-M groups with PA treatment (Fig. 1A and B). As shown by western blot analysis, the protein levels of p-AMPK increased considerably only at 100 ng/mL and 1 μg/mL in the JRG-M group as compared to the control ($p < 0.001$) (Fig. 1C). In the JRG-M group with PA treatment, hepatic protein levels of SREBP-1c were significantly decreased at every concentration as compared to the control ($p < 0.001$) while decreased at 100 ng/mL and 1 μg/mL in the JRG-S group. The protein levels of FAS were significantly diminished by treating only the JRG-M in a dose-dependent manner, but not the JRG-S. Furthermore, diminished mRNA expressions of LXRβ, but not LXRα, were observed at 1 μg/mL in the JRG-M group with PA treatment ($p < 0.01$) (Fig. 1D). Hepatic mRNA levels of C/EBPα were significantly reduced at every concentration in both the JRG-S and JRG-M groups with PA treatment ($p < 0.001$). ACCα, ACCβ, and LPL mRNA levels were also decreased in the JRG-S or JRG-M group with PA treatment. According to these results, JRG-S or JRG-M could alleviate the PA-induced lipid metabolism response by modulation of lipogenesis.

3.3. JRG-S or JRG-M decreased PA-induced inflammation and oxidative stress in single cultured cells

The mRNA expression levels of TNF-α, IL-6, or IL-1β were significantly diminished in PA-treated AML-12 cells (Fig. 2A) or RAW 264.7 cells (Fig. 2B) that had been treated with either JRG-S or JRG-M, except for IL-1β in RAW 264.7 cells. The protein levels of TNF-α in RAW 264.7 cells, macrophage cells regulating immune response, were reduced at 1 μg/mL in the JRG-S group and at 100 ng/mL and 1 μg/mL in the JRG-M group with PA treatment. The IL-6 levels were decreased at 1 μg/mL in the JRG-S and at 10 ng/mL in the JRG-M groups with PA treatment, as compared to the control (Fig. 2C). Hepatic mRNA levels of HO-1 were increased at 100 ng/mL in the JRG-M group with PA treatment (Fig. 2D). These results indicate that JRG-S or JRG-M relieve PA-induced inflammatory responses and could reduce oxidative stress, as well as lipid metabolism.

3.4. JRG-S or JRG-M regulated the expression of NASH-related markers in co-cultured cells

To estimate the effects of JRG-S or JRG-M in an environment similar to an *in vivo* liver condition in which hepatocytes and macrophages coexist, PA-treated AML-12 cells and RAW 264.7 cells were co-cultured with or without JRG-S or JRG-M treatment for 24 hours. In co-cultured AML-12 cells, TNF-α mRNA expressions were decreased in both of the JRG-S and JRG-M groups with PA treatment, but IL-1β was significantly diminished only in the JRG-M group with PA treatment (Fig. 2E). The mRNA expression of TNF-α was significantly diminished at 1 μg/mL in both JRG-S and JRG-M groups, and IL-1β was considerably decreased at every concentrations in JRG-S and JRG-M groups in co-cultured RAW 264.7 cells

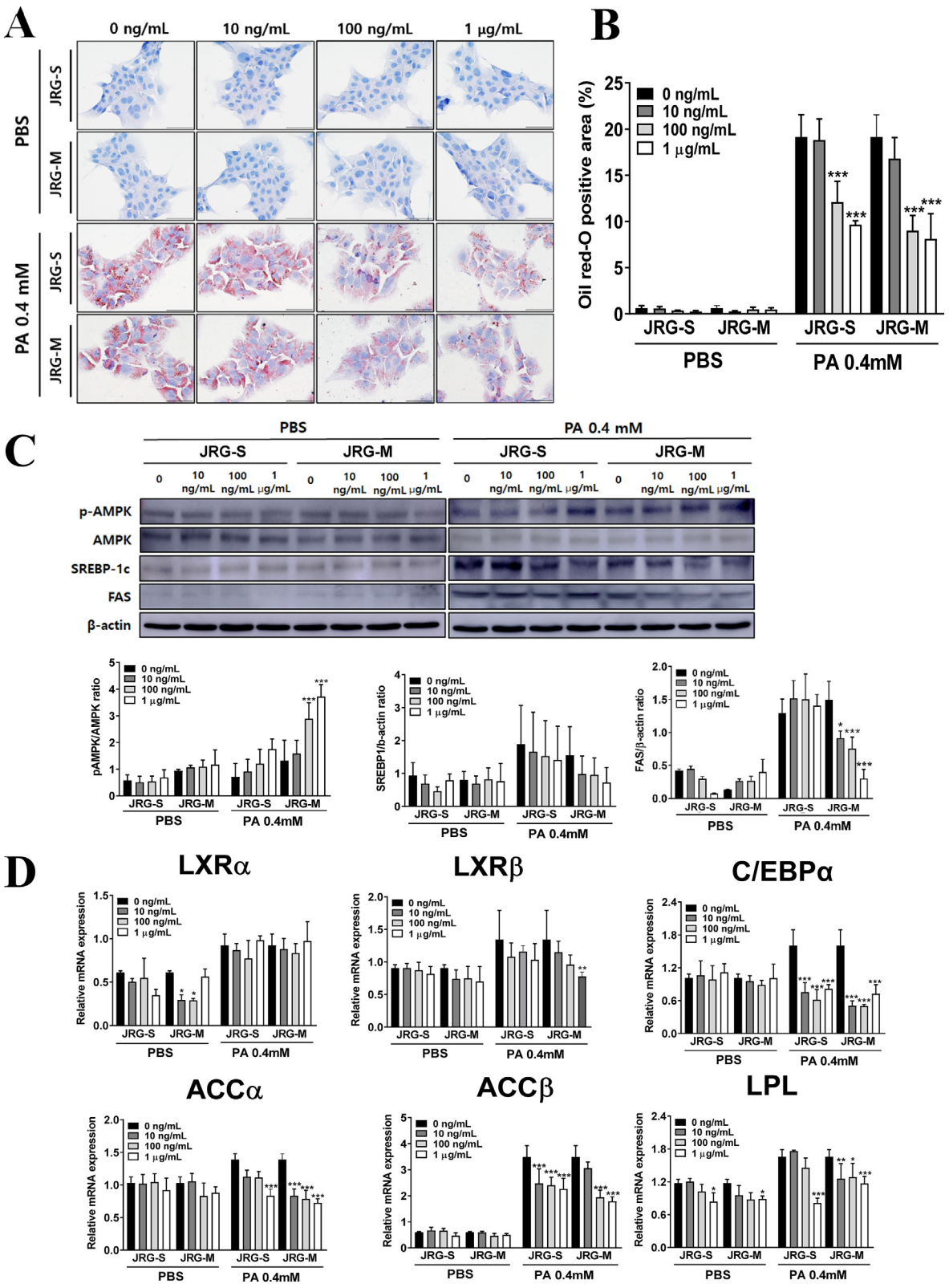

Fig. 1. JRG-S and JRG-M alleviate PA-induced NASH via modulation of lipogenesis *in vitro,* (A and B) Oil Red-O stained liver section's representative images are shown with its positive area in AML-12 cells (scale bar: 35 μm). (C) Protein levels of p-AMPK, AMPK, SREBP-1c, FAS, and β-actin in AML-12 cells and their relative protein intensity are measured with a western blot analysis. (D) Hepatic mRNA level of lipid metabolism-associated genes was assayed by qRT-PCR analysis in AML-12 cells. The graph indicates the expression level against GAPDH. All statistics were done by comparing the control group of each group. *$p < 0.05$, **$p < 0.01$, ***$p < 0.001$.

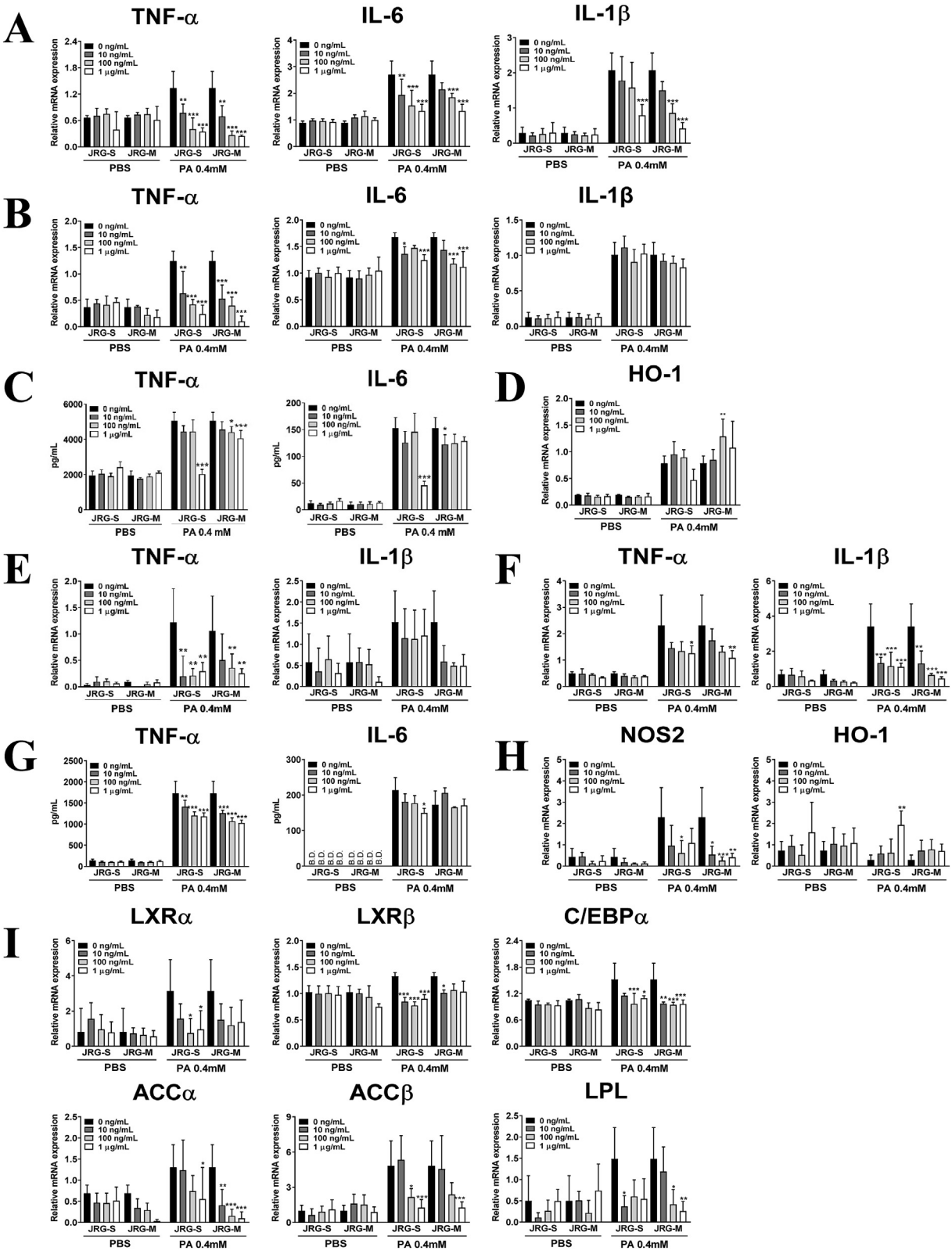

Fig. 2. JRG-S and JRG-M modulated the expression of NASH-related markers in both single cultured and co-cultured cells. The mRNA expressions of TNF-α, IL-6, and IL-1β were measured with qRT-PCR in (A) AML-12 cells or (B) RAW 264.7 cells, and (C) the protein levels of TNF-α or IL-6 were detected with ELISA in the RAW 264.7 cells. The lowest minimal measurable value of the detection kit was expressed as "below the detection limit (B.D.)". (D) The oxidative stress factor levels were assessed in AML-12 cells with qRT-PCR. The mRNA expressions of TNF-α and IL-1β were measured with qRT-PCR in co-cultured (E) AML-12 cells or (F) RAW 264.7 cells, and (G) hepatic TNF-α or IL-6 protein levels were detected with ELISA in cell supernatants. (H) Oxidative stress factor levels and (I) lipid metabolism-related factors were assayed in co-cultured AML-12 cells with qRT-PCR. The graph indicates the expression level against GAPDH. All statistics were done by comparing the control group of each group. $*p < 0.05$, $**p < 0.01$, $***p < 0.001$.

with PA treatment (Fig. 2F). We also observed diminished protein levels of TNF-α and IL-6 in cell supernatants in the JRG-S and JRG-M groups with PA treatment (Fig. 2G). NOS2 mRNA levels were significantly decreased at 1 μg/mL in JRG-S and every concentrations in JRG-M groups with PA treatment, whereas HO-1 was increased at 1 μg/mL only in the JRG-S group (Fig. 2H). Moreover, decreased mRNA expressions of LXRα, LXRβ, C/EBPα, ACCα, ACCβ, and LPL were observed in the JRG-S and JRG-M groups with PA treatment (Fig. 2I). Taken together, these findings indicate that JRG-S and JRG-M treatment diminishes NASH severity, owing to decreased inflammation, fibrosis, and oxidative stress in co-cultured AML-12 cells and RAW 264.7 cells with PA treatment.

3.5. JRG-S or JRG-M administration ameliorates WD-induced liver injury

Morphologically, livers from WD-administrated mice that had had treatment of high concentration of JRG-S or JRG-M were significantly reduced in size, and they were reddish-brown in color as compared to the WD-fed control group, which were pale in color and of a large size (Fig. 3A). We also visually confirmed that the amount of abdominal fat had been decreased by the administration of JRG-S and JRG-M. The body weight, liver weight, and liver/body ratio were decreased by JRG-S and JRG-M administration (Fig. 3B). The serum AST levels were also remarkably decreased in the M 400 group ($p < 0.05$) and ALT levels were significantly diminished in the S 400, M 200 and M 400 groups ($p < 0.01$) as compared to the WD control group (Fig. 3C). Hepatic TG levels were slightly, but significantly, diminished at the highest concentration in both the JRG-S and JRG-M groups, and TC levels were remarkably diminished in the WD-fed mice that had been administered JRG-S or JRG-M (Fig. 3D). These findings collectively suggest that NASH-induced liver injuries are diminished by JRG-S or JRG-M administration.

3.6. JRG-S or JRG-M administration ameliorates the severity of NASH

WD-fed mice that received JRG-S or JRG-M showed reduced NAS score. These were the aggregated scores from histopathologic lesion such as steatosis, lobular inflammation, and hepatocyte ballooning degeneration in H&E staining (Fig. 4A and B). WD-fed mice administered JRG-S or JRG-M showed significantly lower lipid accumulation in the liver, founded on Oil Red-O staining and its positive area measurements (Fig. 4C and D). As shown in Fig. 4E and F, significantly lower positive areas in the liver indicate that collagen distribution was decreased by JRG-S or JRG-M administration. Moreover, a lower number of apoptotic cells was found in WD-fed mice that had been administered JRG-S or JRG-M as compared to the WD control group, except for the S 50 and the S 100 groups, as revealed by TUNEL assay (Fig. 4G and H). Collectively, JRG-S or JRG-M mitigates the severity of NASH, based on pathologic processes including inflammation, liver fibrosis, and cellular injury.

3.7. JRG-S or JRG-M administration decreased hepatocellular lipid metabolism induced by WD feeding

Consistent with *in vitro* results, a ratio of p-AMPK/AMPK levels was markedly increased in the M 200 and M 400 groups. The level in the SREBP-1c was significantly decreased in all groups having JRG-S and JRG-M administration in all WD-fed mice (Fig. 5A). In the M 200 and M 400 groups that had been fed with a WD, the expression of FAS protein was markedly diminished. Furthermore, JRG-S and JRG-M administration diminished the mRNA expression levels of lipogenic ACCα, ACCβ, LPL, LXRα, and LXRβ, but the level of C/EBPα was only diminished in the JRG-M group (Fig. 5B). This data suggests that treatment with JRG-S and JRG-M inhibits the expression of downstream molecules, like SREBP-1c and FAS, which are modulated by AMPK activation in lipid metabolism and which diminish *de novo* lipogenesis in the NASH model.

3.8. JRG-S or JRG-M administration decreased NASH-related hepatocellular inflammation, fibrosis, and oxidative stress

Administration of JRG-S significantly reduced the hepatic mRNA levels of TNF-α in the S 400 group as well as IL-6 in the S 200 and S 400 groups, as compared to the WD group (Fig. 6A). JRG-M also reduced TNF-α and IL-1β mRNA levels in the M 400 group considerably, as well as IL-6 in every group as compared to the WD control group. In the S 200, S 400, and M 400 groups, decreased mRNA expression levels of Col 1 were observed (Fig. 6B), and mRNA levels of α-SMA were diminished in the M 200 and M 400 groups. As shown in Fig. 6C, hepatic mRNA expression levels of NOS2 were significantly decreased in all JRG-S and JRG-M groups, and that of HO-1 was increased in S 200, S 400, and M 400 groups. Therefore, JRG-S or JRG-M affects NASH progression in various NASH-related markers *in vivo* as well as *in vitro*.

4. Discussion

NASH is known to be caused by diverse risk factors, including genetic or environmental factors, lipid accumulation in the liver, insulin resistance, oxidative stress, and mitochondrial dysfunction. To understand the pathogenesis of NASH, the establishment of an optimal NASH model should be the first step. The diet-induced animal model of nonalcoholic fatty liver disease (DIAMOND) that we used in this study is induced by a western diet, including the high-fructose and glucose water *ad libitum* [21], which subsequently causes steatosis, NASH, cirrhosis, and even liver cancer [23]. Therefore, the DIAMOND model has been widely used in recent years among various rodent NASH models because it shows similar patterns to human NASH pathologies, such as steatosis, hepatocellular ballooning, lobular inflammation, and fibrotic progression [23,24].

Phosphorylated AMPK inhibits the expression of SREBP-1c, which is abundantly expressed in liver tissue, thereby reducing the expression of its downstream target genes like FAS, stearoyl-CoA desaturase, and acetyl-CoA carboxylase related to triglyceride synthesis [25,26]. In this study, we found that treatment of JRG-S or JRG-M increased the protein level ratio of p-AMPK/AMPK and consequently reduced the expression of SREBP-1c-target genes. In particular, the protein levels of the FAS were not significantly changed in the JRG-S group, whereas they were significantly diminished in the JRG-M group both *in vivo* and *in vitro*. Therefore, we found that JRG-M alleviates NASH severity via inhibiting lipogenesis with the AMPK-SREBP-1c-FAS pathway. In the case of JRG-S, one study has already demonstrated that JRG extracts inhibit triglyceride synthesis via LXR-SCD expression regulation in HepG2, the human hepatoma cell line [14]. Anti-steatotic effects of JRG-S might be mediated by modulating other AMPK-SREBP-1c downstream, such as low-density lipoprotein receptor or stearoyl-CoA desaturase-1 [27].

The inflammatory response plays a major role in the pathogenesis of NASH. Among various types of hepatic immune cells, KCs located in the hepatic sinusoid are known to be pivotal for regulating the inflammatory responses in steatohepatitic livers [28]. Therefore, modulation of the inflammatory signaling pathway in KCs, as well as hepatocytes, might be a promising therapeutic strategy in patients with NASH. Since it is difficult to isolate cells from humans for *in vitro* experiments, studies using cell lines are being alternatively conducted. Giridhar Kanuri and Ina Bergheim

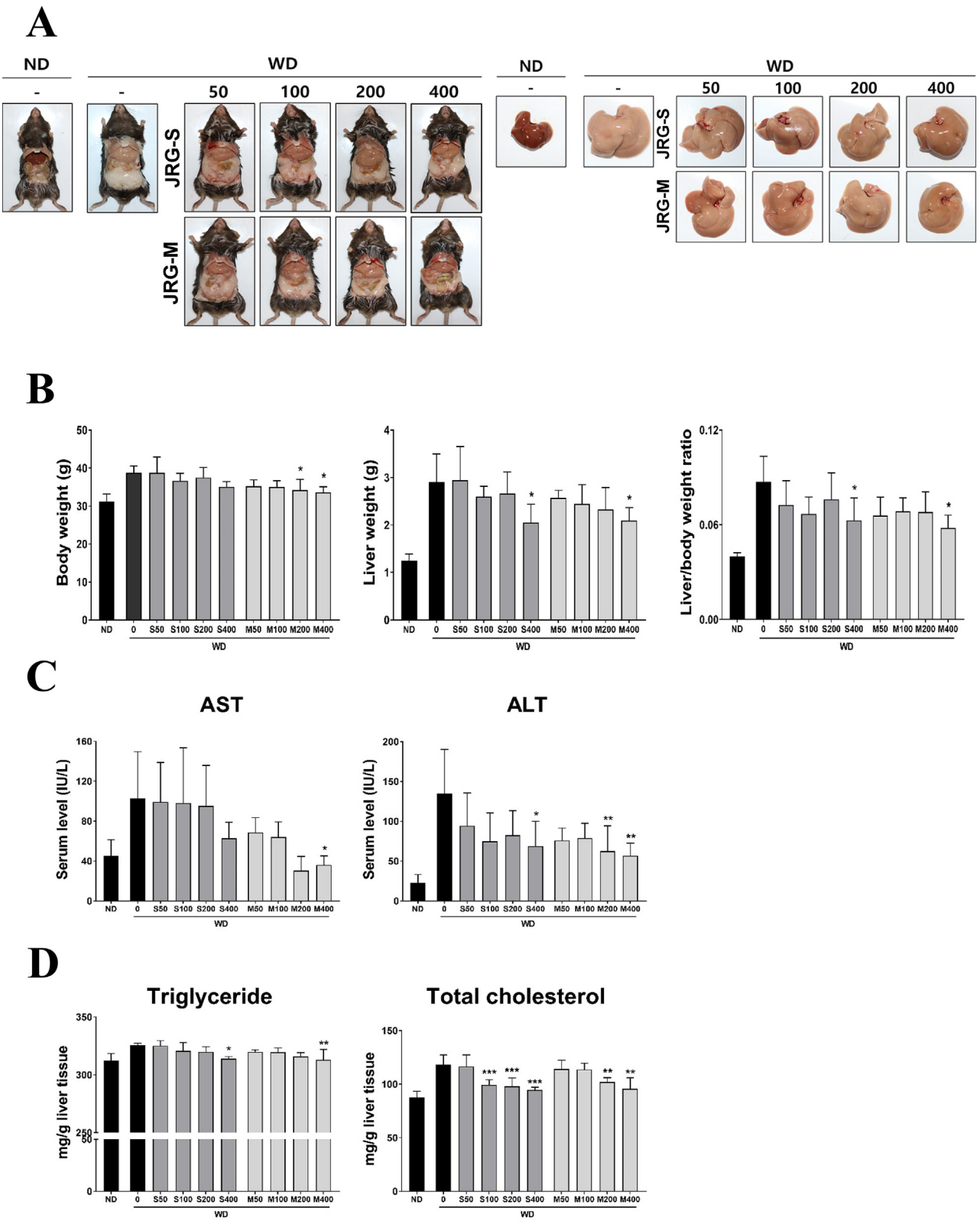

Fig. 3. JRG-S and JRG-M administration affected NASH progression in WD-fed mice. (A) Representative images of liver morphology and (B) body weight, liver weight, and liver/body ratio are shown. (C and D) Serum and hepatic biochemical activity is measured in order to evaluate NASH-associated liver injury and lipid accumulation. All statistics were done by comparing the control group of each group. *$p < 0.05$, **$p < 0.01$, ***$p < 0.001$.

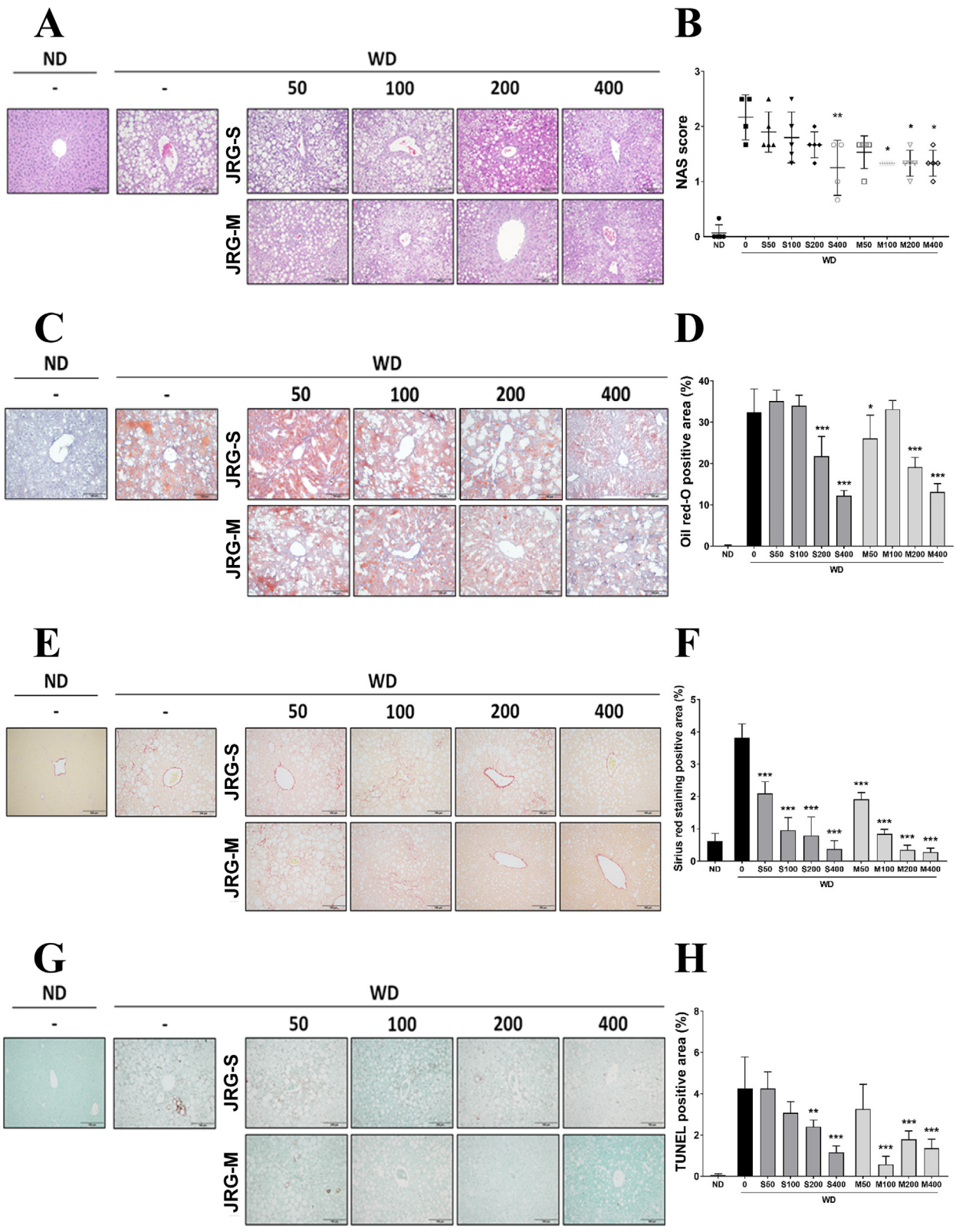

Fig. 4. JRG-S and JRG-M administration improved NASH in WD-fed mice based on histological changes. Representative microscopic images showed (A) H&E, (C) Oil Red-O, (E) sirius red, and (G) TUNEL-stained liver sections from WD-fed mice with or without JRG-S and JRG-M administration (scale bar: 100 μm) (B) NAS scoring and (D, F, and H) the positive areas of each staining were evaluated. All statistics were done by comparing the control group of each group. *$p < 0.05$, **$p < 0.01$, ***$p < 0.001$.

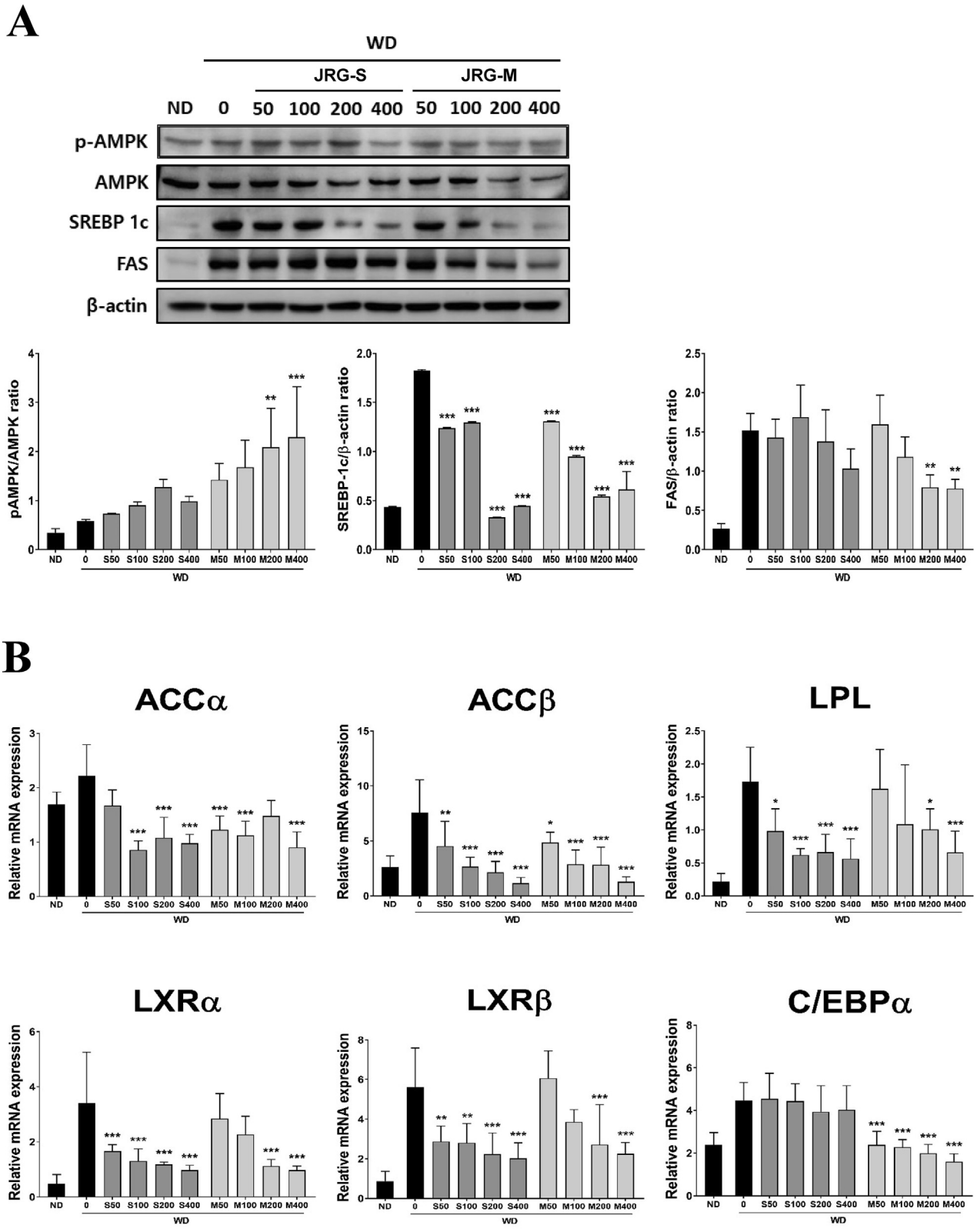

Fig. 5. JRG-S and JRG-M modulated NASH-related lipid metabolism in WD-fed mice. (A) Western blot analysis of lipid metabolism-related proteins and their relative protein intensities were done for NASH-induced mice liver tissue. (B) Hepatic mRNA levels of lipid metabolism-related genes were measured. All statistics were done by comparing the control group of each group. $*p < 0.05$, $**p < 0.01$, $***p < 0.001$.

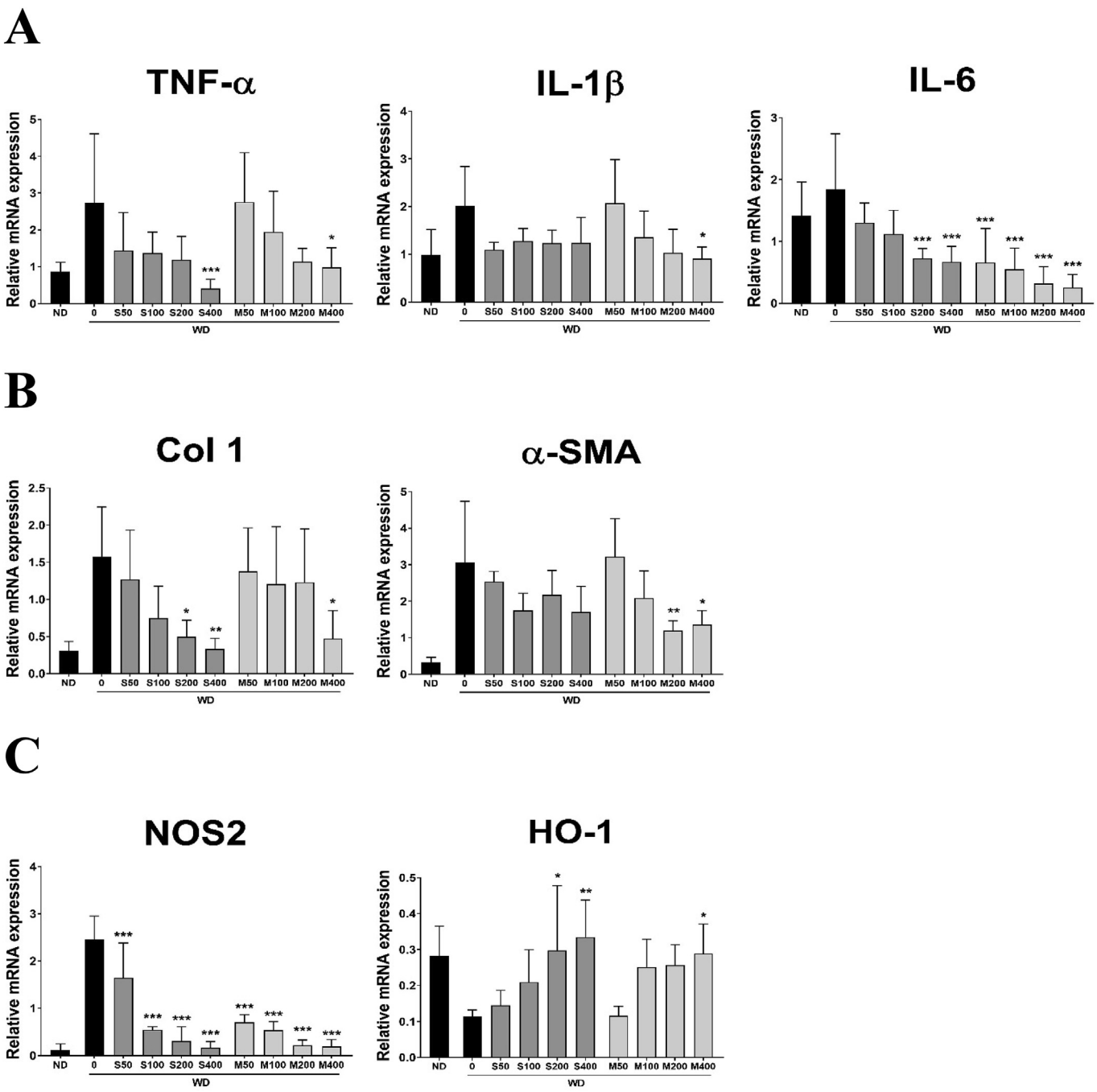

Fig. 6. Administration of JRG-S and JRG-M downregulated the expression of NASH-related proinflammatory cytokines, fibrogenic, and oxidative stress genes. Hepatic mRNA expressions of (A) proinflammatory cytokines, (B) fibrogenic, and (C) oxidative stress genes were assessed by qRT-PCR in the livers of each group. All statistics were done by comparing the control group of each group. *$p < 0.05$, **$p < 0.01$, ***$p < 0.001$.

have shown that RAW 264.7 cells and KCs show similar reactivity against stimuli [29]. Therefore, AML-12 cells and RAW 264.7 cells to perform *in-vitro* single or co-culture NASH models can be replaced as alternative cells for primary hepatocytes and KCs. Thus, we used herein AML-12 cells and RAW 264.7 cells and found a positive induction response to PA treatment, providing an appropriate NASH *in vitro* disease model. In this paper, we confirmed that increased mRNA level of inflammatory cytokines by PA was remarkably decreased by treatment with JRG-S or JRG-M. Furthermore, similar results were observed in co-culture experiments using AML-12 and RAW 264.7 cells to mimic *in vivo* NASH pathogenesis.

Herbal medicines such as JRG and licorice, are preferred because they are more easily accessible than are other chemically synthetic treatments. Thus, these ingredients can be suggested as alternative medicines without toxicity by using the appropriate concentrations. The content of JRG components greatly influenced by the manufacturing method, and the content of ginsenoside increases with the age of JRG [30,31]. In comparison to fresh ginseng, JRG,

which undergoes a steaming process, has higher pharmacological activity and stability due to changes in chemical components [32,33]. Because of these points, JRG has the strict manufacturing process and management to maintain its effectiveness. Among various ingredients in licorice, glycyrrhizin has been demonstrated to have hepatoprotective effects in lipopolysaccharide, carbon tetrachloride, or alcohol-induced liver injury models [34–36]. In this study, we combined a new mixture at a 7:3 ratio of JRG to licorice, showing the highest cell viability in PA-treated AML-12 cells. This showed antiinflammatory and antisteatotic effects in the NASH model. Recently, various studies have been striving to develop a complex treatment by mixing ingredients known to have disease-relieving effects [15–18]. These attempts may address the limited supply of existing ingredients and lead to the development of new health functional foods.

Regarding each component's proportion in the mixture used in this study, JRG-S was 100% of the JRG, and JRG-M was 70%, along with 30% licorice. Hence, it is difficult to clarify the synergistic effects of JRG and licorice because of their different proportions. Nevertheless, JRG-M-treated cells in the NASH milieu showed lower mRNA expression levels of LXRβ, ACCα, LPL, and IL-1β than did the JRG-S-treated cells. Furthermore, the bodyweight, serum biochemicals, and the mRNA expression levels of C/EBPα, IL-1β, IL-6, and α-SMA were remarkably reduced in the WD-fed mice treated with a high dose JRG-M as compared to the JRG-S-treated mice. These results indicate that JRG-M show similar or improved alleviation effects on NASH severity, despite its lower amounts of JRG compared to JRG-S. Therefore, we thought that JRG-M might be more effective than JRG-S. In addition to its-beneficial effects on NASH progression, JRG-M seems more cost-effective than other herbal mixtures because of its relatively simple manufacturing process. Overall, we hope that JRG-M can be widely used as a prophylactic or alternative treatment for NASH.

Declaration of competing interest

The authors declare that there are no conflicts of interest.

Acknowledgments

This study was supported by the Ministry of Agriculture, Food and Rural Affairs (MAFRA), through the 2015 Healthy Local Food Branding Project of the Rural Resources Complex Industrialization Support Program.

Appendix A. Supplementary data

Supplementary data to this article can be found online at https://doi.org/10.1016/j.jgr.2021.05.006.

References

[1] Raffaele M, Licari M, Amin S, Alex R, Shen HH, Singh SP, Vanella L, Rezzani R, Bonomini F, Peterson SJ. Cold press pomegranate seed oil attenuates dietary-obesity induced hepatic steatosis and fibrosis through antioxidant and mitochondrial pathways in obese mice. Int J Mol Sci 2020;21:5469.
[2] Neuschwander-Tetri BA, Caldwell SH. Nonalcoholic steatohepatitis: summary of an AASLD single topic conference. Hepatology 2003;37:1202–19.
[3] Bugianesi E, Leone N, Vanni E, Marchesini G, Brunello F, Carucci P, Musso A, De Paolis P, Capussotti L, Salizzoni M, et al. Expanding the natural history of nonalcoholic steatohepatitis: from cryptogenic cirrhosis to hepatocellular carcinoma. Gastroenterology 2002;123:134–40.
[4] Wree A, Broderick L, Canbay A, Hoffman HM, Feldstein AE. From NAFLD to NASH to cirrhosis-new insights into disease mechanisms. Nat Rev Gastroenterol Hepatol 2013;10:627–36.
[5] Chen X, Xue H, Fang W, Chen K, Chen S, Yang W, Shen T, Chen X, Zhang P, Ling W. Adropin protects against liver injury in nonalcoholic steatohepatitis via the Nrf2 mediated antioxidant capacity. Redox Biol 2019;21:101068.
[6] Li H, Zhou Y, Wang H, Zhang M, Qiu P, Zhang M, Zhang R, Zhao Q, Liu J. Crosstalk between liver macrophages and surrounding cells in nonalcoholic steatohepatitis. Front Immunol 2020;11.
[7] Song K, Kwon H, Han C, Chen W, Zhang J, Ma W, Dash S, Gandhi CR, Wu T. Yes-associated protein in kupffer cells enhances the production of proinflammatory cytokines and promotes the development of nonalcoholic steatohepatitis. Hepatology 2020;72:72–87.
[8] Kim JH. Cardiovascular diseases and Panax ginseng: a review on molecular mechanisms and medical applications. J Ginseng Res 2012;36:16–26.
[9] Seo SJ, Cho JY, Jeong YH, Choi YS. Effect of Korean red ginseng extract on liver damage induced by short-term and long-term ethanol treatment in rats. J Ginseng Res 2013;37:194–200.
[10] Heo SB, Lim SW, Jhun JY, Cho ML, Chung BH, Yang CW. Immunological benefits by ginseng through reciprocal regulation of Th17 and Treg cells during cyclosporine-induced immunosuppression. J Ginseng Res 2016;40:18–27.
[11] Hong M, Lee YH, Kim S, Suk KT, Bang CS, Yoon JH, Baik GH, Kim DJ, Kim MJ. Anti-inflammatory and antifatigue effect of Korean Red Ginseng in patients with nonalcoholic fatty liver disease. J Ginseng Res 2016;40:203–10.
[12] Sung KS, Chun C, Kwon YH, Kim KH, Chang CC. Effects of red ginseng component on the antioxidative enzymes activities and lipid peroxidation in the liver of mice. J Ginseng Res 2000;24:29–34.
[13] Kim SH, Kang JS, Lee SJ, Chung YJ. Antidiabetic effect of Korean red ginseng by puffing process in streptozotocin-induced diabetic rats. J Korean Soc Food Sci Nutr 2008;37:701–7.
[14] Hwang SM, Park CB. Jinan red ginseng extract inhibits triglyceride synthesis via the regulation of LXR-SCD expression in hepatoma cells. Korean J Food Sci Technol 2019;51:558–64.
[15] Choi YH, Kim SE, Huh J, Han YH, Lee MJ. Antibacterial and antioxidative activity of roasted coffee and red ginseng mixture extracts. J Korean Soc Food Sci Nutr 2012;41:320–6.
[16] Choi ME, Jeon BK, Kim DS, Mun YJ, Woo WH. A study on application for beauty food of mixture of Korean red ginseng and Fagopyrum esculentum: antioxidative effect and collagenase inhibitory activity. Herb Formula Sci 2009;17:153–62.
[17] Zheng Y, Lee EH, Lee JH, In G, Kim J, Lee MH, Lee OH, Kang IJ. Preclinical research on a mixture of red ginseng and licorice extracts in the treatment and prevention of obesity. Nutrients 2020;12:2744.
[18] Lee SK, So SH, Hwang EI, Koo BS, Han GH, Ko SB, Kim NM. Effect of ginseng and herbal plant mixtures on anti-obesity in obese SD rat induced by high fat diet. J Korean Soc Food Sci Nutr 2008;37:437–44.
[19] Ram A, Mabalirajan U, Das M, Bhattacharya I, Dinda AK, Gangal SV, Ghosh B. Glycyrrhizin alleviates experimental allergic asthma in mice. Int Immunopharmacol 2006;6:1468–77.
[20] Zhou Z, Kim JW, Zhao J, Qi J, Choi SJ, Lim CW, Lee MY, Lee K, Kim B. Treatment of cigarette smoke extract and condensate differentially potentiates palmitic acid-induced lipotoxicity and steatohepatitis in vitro. Toxicol In Vitro 2018;52:33–40.
[21] Asgharpour A, Cazanave SC, Pacana T, Seneshaw M, Vincent R, Banini BA, Kumar DP, Daita K, Min HK, Mirshahi F. A diet-induced animal model of non-alcoholic fatty liver disease and hepatocellular cancer. J Hepatol 2016;65:579–88.
[22] Kleiner DE, Brunt EM, Van Natta M, Behling C, Contos MJ, Cummings OW, Ferrell LD, Liu YC, Torbenson MS, Unalp-Arida A. Design and validation of a histological scoring system for nonalcoholic fatty liver disease. Hepatology 2005;41:1313–21.
[23] Febbraio MA, Reibe S, Shalapour S, Ooi GJ, Watt MJ, Karin M. Preclinical models for studying NASH-driven HCC: how useful are they? Cell Metab 2019;29:18–26.
[24] Towler MC, Hardie DG. AMP-activated protein kinase in metabolic control and insulin signaling. Circ Res 2007;100:328–41.
[25] Shimomura I, Shimano H, Horton JD, Goldstein JL, Brown MS. Differential expression of exons 1a and 1c in mRNAs for sterol regulatory element binding protein-1 in human and mouse organs and cultured cells. J Clin Investig 1997;99:838–45.
[26] Horton JD, Goldstein JL, Brown MS. SREBPs: activators of the complete program of cholesterol and fatty acid synthesis in the liver. J Clin Investig 2002;109:1125–31.
[27] Bertolio R, Napoletano F, Mano M, Maurer-Stroh S, Fantuz M, Zannini A, Bicciato S, Sorrentino G, Del Sal G. Sterol regulatory element binding protein 1 couples mechanical cues and lipid metabolism. Nat Commun 2019;10:1–11.
[28] Tran S, Baba I, Poupel L, Dussaud S, Moreau M, Gélineau A, Marcelin G, Magréau-Davy E, Ouhachi M, Lesnik P. Impaired Kupffer cell self-renewal alters the liver response to lipid overload during non-alcoholic steatohepatitis. Immunity 2020;53:627–40. e5.
[29] Kanuri G, Bergheim I. In vitro and in vivo models of non-alcoholic fatty liver disease (NAFLD). Int J Mol Sci 2013;14:11963–80.
[30] Shan SM, Luo JG, Huang F, Kong LY. Chemical characteristics combined with bioactivity for comprehensive evaluation of Panax ginseng CA Meyer in different ages and seasons based on HPLC-DAD and chemometric methods. J Pharm Biomed Anal 2014;89:76–82.
[31] Shi W, Wang Y, Li J, Zhang H, Ding L. Investigation of ginsenosides in different parts and ages of Panax ginseng. Food Chem 2007;102:664–8.
[32] In G, Ahn NG, Bae BS, Lee MW, Park HW, Jang KH, Cho BG, Han CK, Park CK, Kwak YS. In situ analysis of chemical components induced by steaming

between fresh ginseng, steamed ginseng, and red ginseng. J Ginseng Res 2017;41:361–9.
[33] Kim WY, Kim JM, Han SB, Lee SK, Kim ND, Park MK, Kim CK, Park JH. Steaming of ginseng at high temperature enhances biological activity. J Nat Prod 2000;63:1702–4.
[34] Yoshida T, Abe K, Ikeda T, Matsushita T, Wake K, Sato T, Sato T, Inoue H. Inhibitory effect of glycyrrhizin on lipopolysaccharide and d-galactosamine-induced mouse liver injury. Eur J Pharmacol 2007. 576:136-42.
[35] Lee CH, Park SW, Kim YS, Kang SS, Kim JA, Lee SH, Lee SM. Protective mechanism of glycyrrhizin on acute liver injury induced by carbon tetrachloride in mice. Biol Pharm Bull 2007;30:1898–904.
[36] Jung JC, Lee YH, Kim SH, Kim KJ, Kim KM, Oh S, Jung YS. Hepatoprotective effect of licorice, the root of Glycyrrhiza uralensis Fischer, in alcohol-induced fatty liver disease. BMC Complement Altern Med 2015;16:1–10.